An assessment on forced convection in metal foams

2012 J. Phys.: Conf. Ser. 395 012148

(http://iopscience.iop.org/1742-6596/395/1/012148)

An assessment on forced convection in metal foams

S Mancin[1,2] **and L Rossetto**[1]

[1]Dipartimento di Ingegneria Industriale, Università di Padova, Padova 35131, Italia

Abstract. Metal foams are a class of cellular structured materials with open cells randomly oriented and mostly homogeneous in size and shape. In the last decade, several authors have discussed the interesting heat transfer capabilities of these materials as enhanced surfaces for air conditioning, refrigeration, and electronic cooling applications. This paper reports an assessment on the forced convection through metal foams presenting experimental and analytical results carried out during air heat transfer through twelve aluminum foam samples and nine copper foam samples. The metal foam samples present different numbers of pores per linear inch (PPI), which vary between 5 and 40 with a porosity ranging between 0.896-0.956; samples of different heights have been studied. From the experimental measurements two correlations for the heat transfer coefficient and pressure drop calculations have been developed. These models can be successfully used to optimize different foam heat exchangers for any given application.

1. Introduction

Open cell metal foams are a class of cellular structured materials with open cells randomly oriented and mostly homogeneous in size and shape [1] that have high specific surface areas, relative high thermal conductivity and present tortuous flow paths, which promote mixing. In the last decades, several independent research groups have investigated the heat transfer capabilities of metal foams by measuring the heat transfer and fluid flow during single phase forced convection through their porous matrices. Mancin et al. [2] have recently proposed a comprehensive review on this topic.

In order to develop accurate models to describe the heat transfer and fluid flow performance of such complex enhanced surfaces, it is fundamental to understand how each parameter affects the heat transfer phenomenon. One of the most important parameters is the foam finned surface efficiency, which depends on several other factors: the actual heat transfer coefficient, foam height, fiber length and thickness, pore density, porosity and, finally, the foam thermal conductivity.

Unfortunately, relatively poor information about the material effects on the heat transfer performance of metal foams is available in the open literature as most of the measurements regards solely aluminum foams, among them: Calmidi and Mahajan [3], Kim et al. [4], Liu et al. [5], Hsieh et al. [6], Mancin et al. [7-10], Boomsma and Poulikakos [11], and Rahli et al. [12]. Copper foams have been experimentally investigated by: Zhang et al. [13], Zhao et al. [14], Giani et al. [15], and Mancin et al. [2].

This study presents the heat transfer and fluid flow measurements of twenty-one, open-cell, aluminum and copper metal foams, when electrically heated and simultaneously cooled by air flowing through. The different effects of: porosity, pore density, foam core height, and material on the heat transfer capabilities are deeply discussed and analysed.

[2] Corresponding author. E-mail: simone.mancin@unipd.it

2. Experimental procedure

In this section the experimental setup, the data reduction and the metal foam database are briefly presented and discussed.

2.1. Experimental setup

The experimental set up is located at the Dipartimento di Ingegneria Industriale (Building of Fisica Tecnica) of the Università di Padova. This paragraph reports a short description of the experimental test rig; detailed information is given in Mancin et al. [9]. The test rig is an open-circuit type wind tunnel with a rectangular cross section and it has been designed and developed to study the heat transfer and fluid flow of air through different enhanced surfaces.

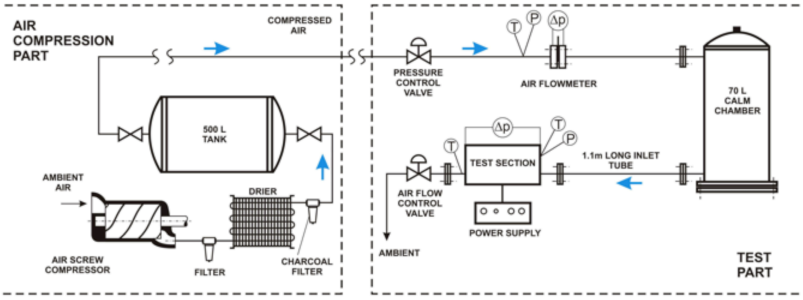

Figure 1. Schematic of the experimental setup.

A schematic of the experimental test rig is reported in figure 1. The ambient air is compressed at a constant gauge pressure of 7 bar and then filtered and blown into a 500 liter air receiver. The compressed air is drawn from the air receiver to the test part. Then, the inlet air is controlled by a pressure control valve located before the orifice volumetric flow meter with an accuracy of ±0.8% of the reading. The air flows into a 70 liter calm chamber and then through the inlet tube to the test section and, finally, it reaches the flow rate control valve and is discharged into the atmosphere.

The test section is made of stainless steel AISI 316L of 300 mm in width, 300 mm in length and 200 mm in height fitted with a suitable Bakelite channel. A detailed description of the test section, which includes the different locations of the thermocouples and pressure taps, is reported in Mancin et al. [9]. A constant heat flux is selected as thermal boundary condition; in fact, the heat flow rate is supplied from the bottom surface of the test sample by means of a copper heater powered by a DC power supply. The samples are cooled by the air, the temperatures of the air at the inlet and outlet of the test section are measured by means of two sets of five (20 mm high samples) or eight (40 mm high samples) calibrated T-type thermocouples. The temperatures are measured using calibrated T-type thermocouples with an accuracy of ±0.05 K; the absolute pressure transducers present an accuracy of ±330 Pa while the differential pressure transducer, located in the test section, has an accuracy of ±2.5 Pa.

2.2. Data reduction

From the experimental measurements it is possible to check the heat balance between the electric power P_{EL} and the air side heat flow rate, calculated as:

$$P_{EL} = \dot{m}_{air} \cdot \bar{c}_{p,air} \cdot \left(t_{air,out} - t_{air,in}\right) \tag{1}$$

where $\dot{m}_{air}$ is the air mass flow rate, $\bar{c}_{p,air}$ the air specific heat at constant pressure and the last term is the air temperature difference between outlet $t_{air,out}$ and inlet $t_{air,in}$ of the test section.

The global heat transfer coefficient *HTC** is defined as the product of the heat transfer coefficient *HTC* and the foam-finned surface efficiency Ω* as:

$$HTC \cdot \Omega^* = \frac{P_{EL}}{A_{base} \cdot \Delta t_{ml}} = HTC^* \tag{2}$$

where the reference surface area, A_{base} is the base area of the test sample and Δt_{ml} is the logarithmic mean temperature difference between the wall and the air temperatures:

$$\Delta t_{ml} = \frac{\left(t_{w,in} - t_{air,in}\right) - \left(t_{w,out} - t_{air,out}\right)}{\ln\left[\frac{\left(t_{w,in} - t_{air,in}\right)}{\left(t_{w,out} - t_{air,out}\right)}\right]} \tag{3}$$

$t_{w,in}$ and $t_{w,out}$ indicate the heated wall temperatures at the inlet and outlet of the base plate, respectively.

The measured pressure drops were rielaborated as suggested in the open literature. Permeability K and the inertia coefficient f are estimated from experimental data. The experimental pressure gradient can be expressed as a function of:

$$\left(-\frac{\mathrm{d}p}{\mathrm{d}z}\right)_{EXP} = \frac{\bar{\mu}}{K}u + \frac{\bar{\rho} \cdot f \cdot u^2}{\sqrt{K}} \tag{4}$$

where u is the air velocity based on the cross section of the empty channel while $\bar{\rho}$ and $\bar{\mu}$ are the dynamic viscosity and the density of the air at the mean temperature and pressure, respectively. This is then rewritten as follows:

$$\left(-\frac{\mathrm{d}p}{\mathrm{d}z}\right)_{EXP} \cdot \frac{1}{u} = \frac{\bar{\mu}}{K} + \frac{\bar{\rho} \cdot f \cdot u}{\sqrt{K}} = a + b \cdot u \tag{5}$$

From a regression analysis, the permeability K and the inertia coefficient f are obtained as:

$$K = \frac{\bar{\mu}}{a} \qquad\qquad f = \frac{b \cdot K^{0.5}}{\bar{\rho}} \tag{6}$$

Finally, the error analyses have pointed out that the heat transfer coefficient presents an average uncertainty of ±1.5% with a maximum value of ±2.5%. Considering the pressure drops, the permeability and inertia coefficient present an uncertainty of 1.0% and 0.7%, respectively.

2.3. Metal foam database

The present paper reports the experimental measurements carried out during air forced convection of twenty-one metal foams. The most important geometrical characteristics of the tested foams are listed in table 1. The metal foam samples are manufactured in a sandwich-like arrangement where the foam core is brazed between two 10 mm thick plates. The specimens are 100 mm long and wide and they present two different foam core heights: 20 mm and 40 mm. Twelve samples are made of aluminum while nine of copper.

The foam structure can be described by porosity ε and the number of pores per inch PPI; the porosity ε is defined as the ratio of total void volume to the total volume occupied by the solid matrix and void volumes, while PPI is easily obtained by counting the number of pores in 25.4 mm. As reported in table 1, samples with 5, 10, 20 and 40 PPI with porosity between 0.896 and 0.956 have been investigated.

Furthermore, the present authors have measured the fiber length l and thickness t, which, as suggested by Gibson and Ashby [1], are useful parameters to describe the structure of the foams and to model their heat transfer and fluid flow behaviours. The fiber thickness t is the mean value of the thickness of the pore's edges while the length of the edge, which connects two adjacent vertices, is considered as the length of the fiber l.

Table 1. Major geometrical characteristics of the tested metal foams.

Sample	Ref	PPI[a]	Porosity[a], ε	Foam Core Height, H	a_{sv} [c]	Fiber thickness[b] t	Fiber length[b], l	Permeability, $K^{b,d}\cdot10^7$	Inertia Coeff., $f^{b,d}$
		[in^{-1}]	[-]	[m]	[$m^2\ m^{-3}$]	[mm]	[mm]	[m^2]	[-]
Al-5-7.9	[7, 8]	5	0.921	0.04	339	0.540	1.959	2.36	0.100
Al-10-4.4	[7, 8]	10	0.956	0.04	537	0.445	1.351	1.82	0.102
Al-10-6.6	[7, 8]	10	0.934	0.04	692	0.450	1.785	1.87	0.082
Al-10-9.7	[7, 8]	10	0.903	0.04	839	0.529	1.870	1.90	0.074
Al-20-6.8	[7, 8]	20	0.932	0.04	1156	0.367	1.218	0.824	0.065
Al-40-7.0	[7, 8]	40	0.930	0.04	1679	0.324	1.072	0.634	0.086
Al-5-8.0	[9]	5	0.920	0.02	342	0.490	1.758	1.52	0.059
Al-10-4.6	[9]	10	0.954	0.02	554	0.385	1.863	2.165	0.108
Al-10-7.4	[9]	10	0.926	0.02	736	0.553	1.950	4.29	0.129
Al-10-10.4	[8]	10	0.896	0.02	866	0.484	1.899	2.65	0.106
Al-20-7.0	[9]	20	0.930	0.02	1169	0.315	1.175	0.535	0.050
Al-40-7.4	[9]	40	0.926	0.02	1721	0.282	1.096	0.297	0.050
Cu-5-6.7	[2]	5	0.933	0.02	299	0.500	1.913	0.97	0.051
Cu-10-6.7	[2]	10	0.933	0.02	698	0.390	1.583	2.09	0.091
Cu-10-9.5	[2]	10	0.905	0.02	831	0.403	1.378	1.21	0.056
Cu-20-6.7	[2]	20	0.933	0.02	1148	0.293	1.236	0.41	0.039
Cu-40-6.6	[2]	40	0.934	0.02	1635	0.262	1.109	0.44	0.060
Cu-5-6.5	[-]	5	0.935	0.04	292	0.495	1.890	4.19	0.117
Cu-10-6.6	[-]	10	0.934	0.04	692	0.432	1.739	2.58	0.103
Cu-20-6.5	[-]	20	0.935	0.04	1134	0.320	1.402	1.77	0.123
Cu-40-6.4	[-]	40	0.936	0.04	1611	0.244	0.999	4.50	0.221

[a] Measured by the manufacturer.
[b] Measured by the present authors.
[c] a_{sv}: surface area per unit of volume.
[d] Calculated at mean air temperature and pressure.

3. Results and modelling

In this section the experimental results carried out during air forced convection through the twenty-one aluminum and copper foams are presented in terms of global heat transfer coefficient, interstitial heat transfer coefficient, and pressure gradient. Furthermore, two new models to predict the heat transfer and fluid flow behaviours of the metal foams are proposed and validated against the present database.

3.1. Heat transfer

The heat transfer results are usually presented in terms of the heat transfer coefficient, which has to be referred to a reference surface; in the case of metal foams, there are two different suitable ways to define this parameter: the first one, which uses the base area, is suggested by equation (2); the latter refers to the overall heat transfer area of the metal foam, as:

$$\alpha^* = \alpha \cdot \Omega^* = \frac{HTC^*}{1 + a_{sv} \cdot H} \tag{7}$$

This heat transfer coefficient can be considered as the product of the interstitial heat transfer coefficient and the foam finned surface efficiency. Using these two definitions, it is possible to highlight different thermal aspects, as reported in figures 2-5.

Globally, the heat transfer measurements were carried out by imposing three different heat flow rates: 250, 325 and 400 W and by varying the air mass velocity from 2.0 to 7.0 kg m^{-2} s^{-1}. As described in Mancin et al. [2, 7-10], the heat transfer coefficient does not depend on the imposed heat flux; therefore, for the sake of clarity, the results refer to a heat flux of 25 kW m^{-2}. Figures 2 and 3 show the heat transfer coefficient as defined by equation (7) plotted against the air mass velocity G (referred to the cross section of the empty channel) carried out during air forced convection through metal foams with different PPI and foam core height, at constant porosity.

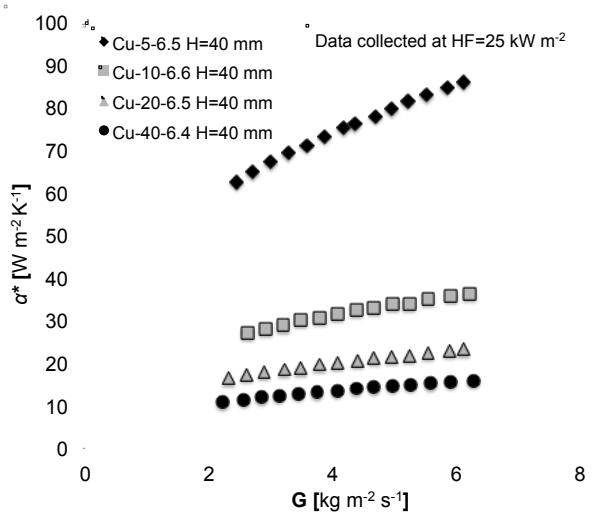

Figure 2. Pore density effect on heat transfer. Data for copper foam at constant porosity.

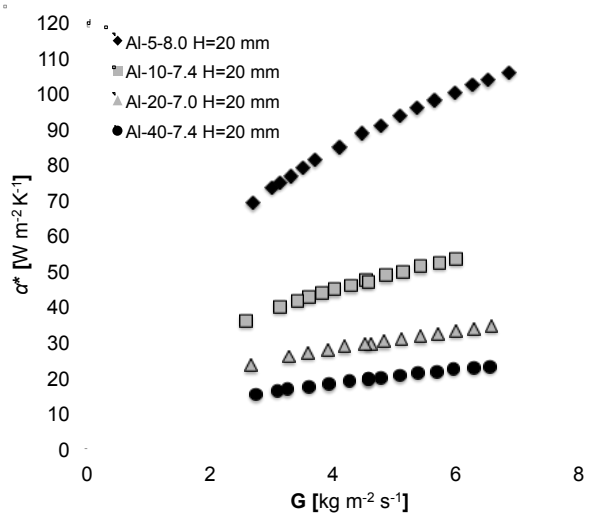

Figure 3. Pore density effect on heat transfer. Data for aluminum foam at constant porosity.

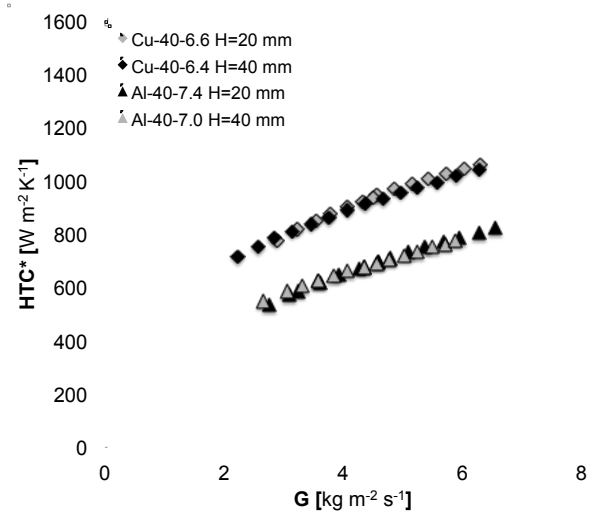

Figure 4. Foam height and material effects on heat transfer. Data for 40 PPI foam samples.

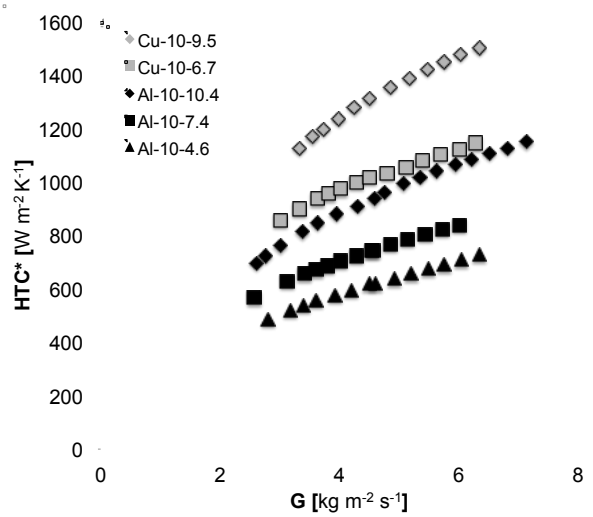

Figure 5. Porosity effect on heat transfer. Data for H= 20 mm metal foams.

As it clearly appears, the heat transfer coefficient increases with the air mass velocity; at constant porosity, it increases when decreasing the pore density (i.e. PPI) for both aluminum and copper foam samples. For instance, looking at figure 2, at G= 4 kg m^{-2} s^{-1}, the heat transfer coefficient of 5 PPI copper foam is 5 times higher than that measured for 40 PPI one; similar considerations can be conducted with regard to aluminum foams (figure 3).

The effect of the foam core height is reported in figure 4 where the global heat transfer coefficient (equation 2) for 40 PPI copper and aluminum foams is plotted against the air mass velocity; first of all, as expected, the copper foams exhibit higher heat transfer performances than those of aluminum foams. Further, the 40 mm high foam samples and the 20 mm high ones show exactly the same global heat transfer coefficients. Considering the copper foams, as listed in table 1, the two samples present almost the same porosity and, thus, similar value of surface area per unit of volume: this means that the 40 mm high foam has double heat transfer area than the 20 mm high one. Since the two specimens show the same global heat transfer coefficient, the foam finned surface efficiency of the 20 mm is somewhat double that of the 40 mm high foam sample. Similar results can be highlighted for all the

tested aluminum and copper foams. Furthermore, the effect of the porosity on the heat transfer performance of metal foams is reported in figure 5, where the global heat transfer coefficient (equation 2) is plotted against the air mass velocity for 20 mm high, copper and aluminum foams, with 10 PPI. It appears that for both copper and aluminum foam samples, the heat transfer performance improves when the porosity decreases.

The heat transfer coefficient defined by equation (7) can be modelled as follows:

$$\alpha = 0.4181 \cdot \mathrm{Re}^{0.5318} \cdot \mathrm{Pr}^{0.333} \cdot \frac{\bar{\lambda}_{air}}{t} \tag{8}$$

The Reynolds number (30 < Re < 200) and the Prandtl number (Pr = 0.7) are defined as:

$$\mathrm{Re} = \frac{G \cdot t}{\varepsilon \cdot \bar{\mu}_{air}} \qquad \mathrm{Pr} = \frac{\bar{\mu}_{air} \cdot \bar{c}_{p,air}}{\bar{\lambda}_{air}} \tag{9}$$

where G is the specific mass velocity, t is the fiber thickness as reported in table 1, ε is the porosity of the foam while $\bar{\mu}_{air}$, $\bar{c}_{p,air}$ and $\bar{\lambda}_{air}$ are the dynamic viscosity, the specific heat at constant pressure and the thermal conductivity evaluated at the mean air temperature and pressure. The foam finned surface efficiency can be calculated using the following equation:

$$\Omega^* = \frac{1 + \Omega \cdot a_{sv} \cdot H}{1 + a_{sv} \cdot H} = \frac{1 + \dfrac{\tanh(m \cdot L)}{m \cdot L} \cdot a_{sv} \cdot H}{1 + a_{sv} \cdot H} \tag{10}$$

the two parameters m and L have been regressed using the experimental database listed in table 1:

$$m = \left(\frac{4 \cdot \alpha}{t \cdot \lambda_{mat}}\right)^{0.5} \left(\frac{\lambda_{mat}}{\bar{\lambda}_{air}}\right)^{-0.5205} \qquad L = 1055 \cdot H^{1.1.75} \cdot PPI \cdot \left(0.0254 - t \cdot PPI\right)^{0.6598} \tag{11}$$

where α is the heat transfer coefficient calculated using equation (8), λ_{mat} is the thermal conductivity of the material, H is the foam core height, t is the fiber thickness and PPI is the pore density. The comparison between the suggested new model and the experimental database shows good agreement: the relative deviation e_R=1.4%, the absolute deviation e_A=6.5% and the standard σ_N=5.1%.

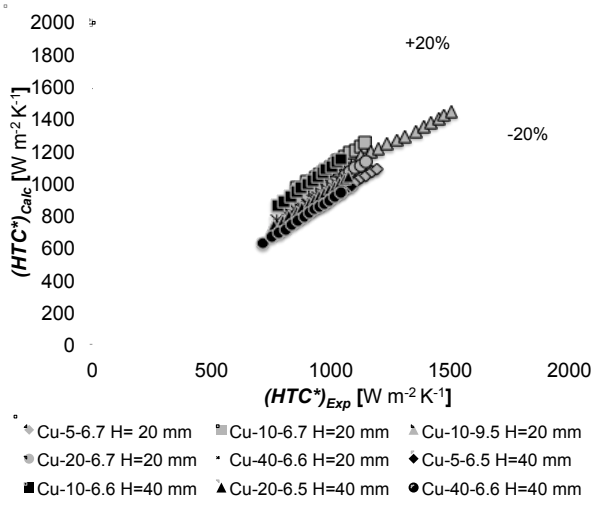

Figure 6. Calculated vs experimental heat transfer coefficients for copper foams data.

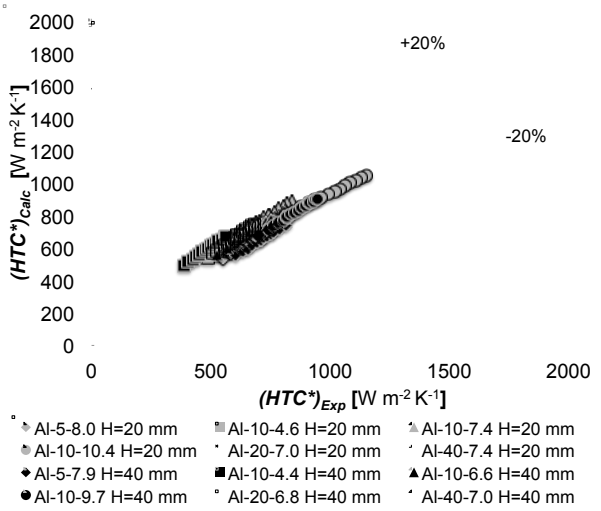

Figure 7. Calculated vs experimental heat transfer coefficients for aluminum foams data.

3.2. Pressure drop

This section discusses the experimental measurements of the pressure drop obtained during the air forced convection through the twenty-one metal foam samples. Table 1 lists the experimental values of permeability and inertia coefficients regressed from the measurements.

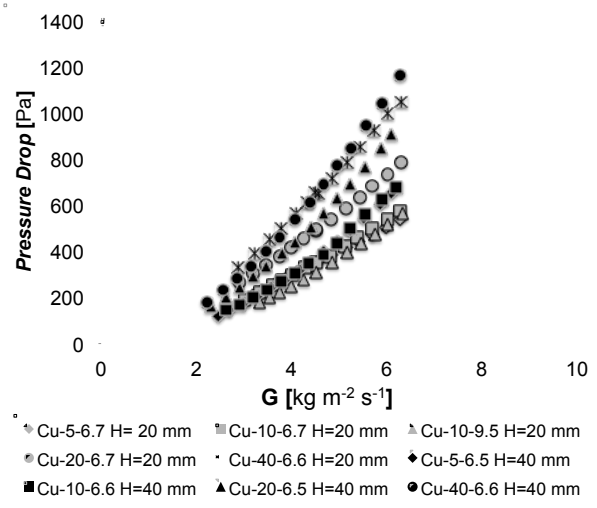

Figure 8. Experimental pressure drop measurements for copper foams data.

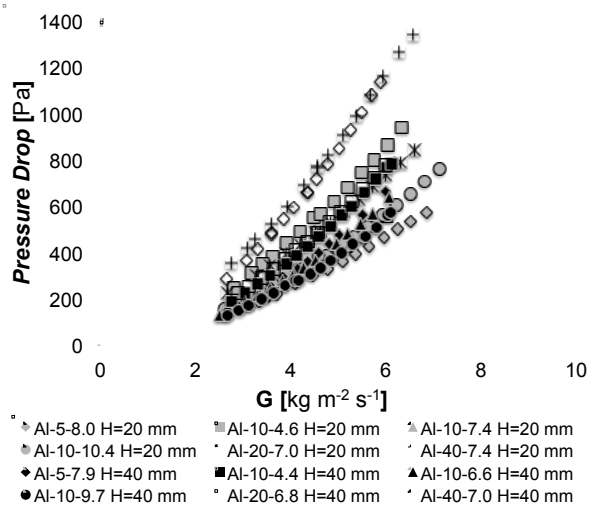

Figure 9. Experimental pressure drop measurements for aluminum foams data.

Figures 8 and 9 show the experimental pressure drop plotted against the air mass velocity; for both metals, the pressure drop increases as the pore density increases and there is not any appreciable effect of the foam core height on the fluid flow behaviour of foams. From the analysis of Figure 9, considering the 40 mm high aluminum foam samples with 10 PPI, the pressure drop increases as the relative density decreases. Mancin et al. [7] proposed a correlation to calculate the pressure drop during air forced convection through metal foams, as follows:

$$\left(\frac{\mathrm{d}p}{\mathrm{d}z}\right) = \frac{2 \cdot F \cdot G^2}{d_h \cdot \bar{\rho}} \tag{12}$$

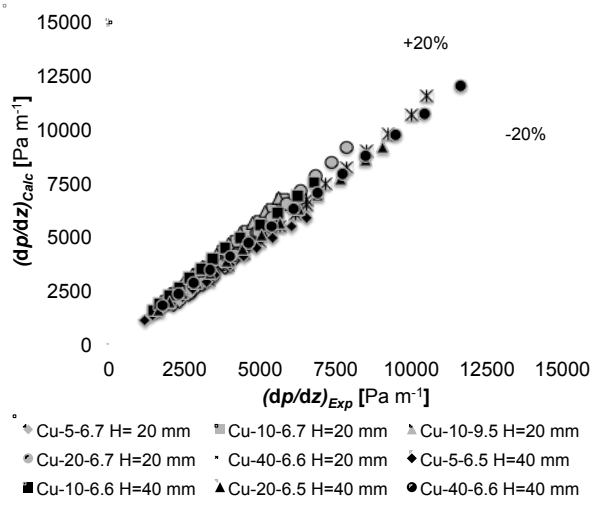

Figure 10. Calculated vs experimental pressure drops for copper foams data.

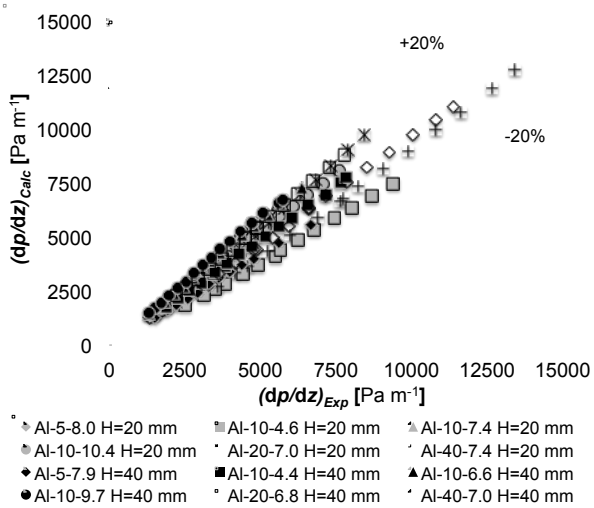

Figure 11. Calculated vs experimental pressure drops for aluminum foams data.

The factor F is expressed as a function of the porosity ($0.896 < \varepsilon < 0.956$), the pore density ($5 < PPI < 40$) and the Reynolds number ($60 < Re < 1250$), as:

$$F = \frac{1.765 \cdot \mathrm{Re}^{-0.1014} \cdot \varepsilon^2}{PPI^{0.6}} = \frac{1.765 \cdot \left(\frac{G \cdot d_h}{\bar{\mu} \cdot \varepsilon} \right)^{-0.1014} \cdot \varepsilon^2}{PPI^{0.6}} \tag{13}$$

The hydraulic diameter for the different metal foams as a function of the pore density:

$$d_h = 0.0122 \cdot PPI^{-0.849} \tag{14}$$

Figures 10 and 11 report the comparison between the suggested model and the experimental values of pressure drop for aluminum and copper foams, respectively. As it appears the model is able to satisfactory predict the experimental measurements within ±20% with a relative deviation of e_R=-1.5%, an absolute deviation of e_A=9.6% and a standard of σ_N =11.4%.

4. Conclusions

This paper presents an assessment on air forced convection through metal foams reporting experimental measurements of heat transfer coefficient and pressure drop carried out by varying the air mass flow rate and the imposed heat flux. The effects of the pore density, porosity, foam core height, and material on the air heat transfer have been encompassed and analysed. From the experimental results, two models, which permit to accurately calculate the heat transfer coefficients and the pressure drops during air flow through metal foams, have been developed and validated. These calculation procedures can be successfully used to optimize different metal foam heat sinks for any kind of electronic thermal management applications.

5. References

[1] Gibson L J and Ashsy M F 1997 *Cellular solids-structures and properties* (Cambridge, UK: Cambridge University Press)
[2] Mancin S, Zilio C, Diani A and Rossetto L 2012 *Exp. Therm. Fluid Sci.* **36** 224-232
[3] Calmidi V V and Mahajan R L 2000 *J. of Heat Transfer* **122** 557-565
[4] Kim S Y, Paek J W and Kang B H 2000 *J. of Heat Transfer* **122**, 572-578
[5] Liu L F, Wu W T, Chiu W C and Hsieh W H, 2006 *Exp. Therm. Fluid Sci.* **30** 329-336
[6] Hsieh W H, Wu J Y, Shih W H and Chiu W C 2004 *Int. J. of Heat and Mass Transf.* **47** 5149-5157
[7] Mancin S, Zilio C, Cavallini A and Rossetto L 2010 *Int. J. of Heat and Mass Transf.* **53** 3121–3130
[8] Mancin S, Zilio C, Cavallini A and Rossetto L 2010 *Int. J. of Heat and Mass Transf.* **53** 4976–4984
[9] Mancin S, Zilio C, Rossetto L and Cavallini A 2011 *J. of Heat Transfer*, **133**, 060904
[10] Mancin S, Zilio C, Rossetto L and Cavallini A 2010 *AIP Conf. Proc. 1254 Porous media and its applications in science, engineering, and industry* pp. 305-310
[11] Boomsma K and Poulikakos D 2002, *ASME J. Fluids Eng.* **124** 263–272.
[12] Rahli O, Tadrist L, Santini R and Pantaloni J 2004 *Exp. Thermal and Fluid Science* **28** (2–3) 193-199
[13] Zhang H Y, Pinjala D, Joshi Y K, Wong T N, Toh K C and Iyer M K 2005 *IEEE Trans. Compon. Pack. Tech.* **28** (2) 272–280
[14] Zhao C Y, Kim T, Lu T J and Hodson H P 2004 *J. Thermophys. Heat Transfer* **18** (3) 309–317
[15] Giani L, Groppi G and Tronconi E 2005 *Ind. Eng. Chem. Res.* **44** 9078–9085